Research Article **Open Access**

Michel P. de Jong*

Recent progress in organic spintronics

DOI 10.1515/phys-2016-0039
Received November 3, 2015; accepted July 1, 2016

Abstract: The field of organic spintronics deals with spin dependent phenomena occurring in organic semiconductors or hybrid inorganic/organic systems that may be exploited for future electronic applications. This includes magnetic field effects on charge transport and luminescence in organic semiconductors, spin valve action in devices comprising organic spacers, and magnetic effects that are unique to hybrid interfaces between (ferromagnetic) metals and organic molecules. A brief overview of the current state of affairs in the field is presented.

Keywords: organic semiconductors; spintronics; organic electronics, magnetism; magnetoresistance; hybrid interfaces

PACS: 72.25.-b; 73.61.Ph; 73.61.Wp; 73.43.Qt; 75.70.Cn; 75.76.+j

1 Introduction

In spintronics [1], information is stored and processed using the spin polarization of electrons and holes, or other (quasi) particles, in electronic devices. Examples of spintronic devices that have been commercialized are giant magnetoresistance devices and magnetic tunnel junctions, best known for their use as hard disk read heads and random access memory cells. Organic electronics utilizes carbon-based, molecular or polymeric semiconductors, which offer low processing costs, mechanical flexibility and, importantly, nearly unlimited chemical tunability of electronic and optical properties [2]. The most widespread commercial organic electronic application is the organic light-emitting device (OLED), which is used in displays (notably in smart phones). Organic spintronics aims to combine these two fields, by bringing organic materials into spintronics, and incorporating spin dependent effects in organic electronics. As will be discussed in this review, this leads to fascinating physics, and tantalizing new opportunities for applications.

The paper is organized as follows: After a brief discussion of spin orbit interaction and hyperfine interaction in organic materials, magnetic field effects on charge transport and luminescence in organic semiconductors are discussed. Subsequently, spin-polarized charge transport in hybrid devices, e.g. spin valves, is addressed. The last section deals with the rich magnetic structure of hybrid interfaces involving organic molecules.

2 Spins in organic materials

2.1 Spin lifetime and spin diffusion length

The interactions between spin-polarized charge carriers and their solid state environment are clearly very important for attaining spin-based functionality in a certain material or heterostructure. This section addresses such interactions, first in general, and then specifically for organic materials. In particular, for many conceptual spintronic devices it is important that the spin orientation of charge carriers remains unperturbed for a sufficiently long time to (i) perform spin operations and readout, or (ii) transport the spins over relevant distances (typically hundreds of nanometers). Important parameters therefore are the *spin lifetime* and *spin diffusion length* [1], which are measures for how long a spin remains unaffected and how far it can travel without being perturbed. Two different time scales are typically defined related to randomization of spins, T_1 and T_2 [1], referring to the time scales for randomization along the spin quantization axis (spin relaxation time) and perpendicular to it (spin dephasing time), respectively. The latter corresponds to the time it takes for an ensemble of spins precessing in phase to lose their phase correlation. The spin diffusion length depends of course on the spin relaxation and dephasing time, but also on the charge carrier mobility. This parameter is therefore not only determined by the interactions between the spins and their environment, but also by the charge transport properties of the material.

***Corresponding Author: Michel P. de Jong:** NanoElectronics Group, MESA+Institute for Nanotechnology, University of Twente, P.O. Box 217, Enschede, 7500AE, The Netherlands, E-mail: M.P.deJong@utwente.nl

2.2 Spin-orbit interaction

The electric fields originating from all nuclei and electrons in a material transform into magnetic fields in the rest frames of the electrons (or holes). The resulting interaction between these magnetic fields and the spin of the electrons is called a spin-orbit interaction (SOI). Since SOI finds its origin in the electric fields of the nuclei (partially screened by electrons), its strength scales strongly with atomic number Z. Organic materials are made up of atoms with low Z, e.g. carbon and hydrogen, such that one might expect the spin orbit coupling to be very weak, and hence insignificant compared to the hyperfine interaction for the randomization of spin orientation. However, its significance should not be dismissed so easily. In fact, several recent works suggests that SOI is important for spin relaxation in organic materials [3–7].

The result of SOI is coupling between the spin and the motion (velocity and direction) of the electron. In solid-state systems featuring electronic bands, e.g. silicon or germanium crystals, the electronic states can be described by Bloch waves. SOI then leads to coupling between the spin and k-vector of the electrons. A result of this is that momentum scattering may also lead to spin flip scattering (Elliot-Yafet mechanism). In addition, spin precession around an SOI-induced magnetic field *in between* scattering events may take place(Dyakonov-Perel mechanism). In organic solids, which are composed of molecules bonded by Van-der-Waals interactions, a description of the electronic states in terms of delocalized bands is generally not applicable. Charge transport takes place by hopping, rather than band-like transport, in most cases even for perfect organic crystals. Some controversy remains regarding the proper description for charge transport in such crystals. It is beyond debate, however, that carrier hopping is the appropriate description for the vast majority of organic semiconductors. Hence, the Elliot Yafet and Dyakonov-Perel mechanisms are not applicable, and modeling of the SOI has to be done with hopping transport in mind.

We point out that SOI in organic semiconductors has been studied previously within the context of the creation and decay of singlet and triplet excitons, relevant for light emitting devices and photovoltaics [8–12]. Recently, several theoretical works have also addressed the role of SOI in relation to spin relaxation for (single carrier) hopping in organic semiconductors [3, 4, 13, 14]. These studies suggest that SOI is indeed important for spin relaxation during polaron hops in certain organic semiconductors, in particular for tris-(8-hydroxyquinoline)aluminum (Alq_3), an extensively studied material in organic spintronics. Experimental support for this notion has been reported, based on muon spin resonance and time-resolved photoluminescence spectroscopy experiments on a series of organic semiconductors containing chemically substituted elements with increasing atomic number [5]. On the other hand, recent reports by Rybicki *et al*. on SOI in conjugated polymer chains suggest that it is negligible in those systems [15, 16]. As has been suggested by Harmon *et al*., further investigation of organic semiconductors with systematic variation of (1) elemental substitution (to obtain different SOI), (2) hopping rates (via temperature or molecular order/disorder) and (3) hyperfine fields (using deuteration) should be performed to shed light on the importance of SOI [13].

2.3 Hyperfine interaction

Due to the presence of (randomly oriented) nuclear magnetic moments in a material, the spin magnetic moments of charge carriers are subjected to a spatially as well as temporally random magnetic field. Electron spin relaxation may take place via electron-nuclear spin flip processes, and dephasing by random precessions in the fluctuating hyperfine fields. These processes have been studied in detail for semiconductor quantum dots, since hyperfine interaction (HFI) is the main source for randomization of electron spins in these systems [17, 18].

Beyond doubt, the hyperfine interaction (HFI) plays an important role in spin relaxation in organic semiconductors. Organic semiconductors are mostly composed of carbon and hydrogen. The most abundant carbon isotope ^{12}C has no nuclear spin, such that the hyperfine fields mostly stem from hydrogen atoms. Since electrons (or holes) in organic semiconductors are in most cases confined to a single molecule (or polymer chain segment), they probe the hyperfine fields of a relatively small number of fluctuating proton spins. Typically, the hyperfine field sensed by an electron scales inversely with the square root of the amount of nuclear spins located within the extent of its wave function [19], which is small for an electron localized on an individual molecule (hence the resulting field is relatively large). Many experimental and theoretical studies have underlined the importance of HFI in magnetic field effects in organic semiconductors, e.g. magnetoresistance and magnetoluminesence (see discussion below). HFI also plays an essential role in magnetic field effects on the kinetics of chemical reactions (intermolecular charge transfer in organic semiconductors is in essence a redox reaction), which is the subject of the spin chemistry field [20].

3 Magnetic field effects in organic semiconductors

The above-discussed coupling between the electron spins and their environment (surrounding charges and nuclear spins) gives rise to very rich magnetic field effects. The influence of magnetic fields on the photoconductivity of antracene and tatracene has been studied since the 1960s [21] Magnetic field effects on the current (magneto-conductance, MC, magnetoresistance, MR) and light output (magnetoluminescence, ML) in organic light emitting devices (OLEDs) have been reported by the groups of Kalinowski [22] and Wohlgenannt [23, 24], and by many others since (see Ref. [25] and references therein). The study of these effects, in particular organic magnetoresistance (OMAR), forms an important sub-field in organic spintronics. In this section, a brief overview of the effects and their proposed origin is discussed, and a few recent studies are highlighted. For a more in depth discussion, the reader is referred to a previously published review [25, 26].

In many organic semiconductors, charge carrier transport and recombination processes are sufficiently influenced by (weak) magnetic fields to produce a noticeable or even large change in (photo)conductance and (electro/photo)luminescence. These effects can be observed in generic organic electronic devices such as OLEDs [22–24] and organic thin-film transistors (OTFTs) [27]. As an example, we take the magnetic field effects observed by Francis et al. (see Fig. 1), in OLEDs based on the conjugated polymer poly(9,9-dioctylfluorenyl-2,7-diyl) (PFO). MR of up to 10% in weak magnetic fields of 10 mT was observed in these devices. Both positive and negative MR values were observed, depending on the bias voltage and choice of the anode/cathode materials. The effects did not show a significant temperature dependence.

Similar MR effects have been reported since then, for a large variety of organic semiconductors (molecular as well as polymeric) by many different research groups [25]. Several generic features of the MR effect can be pointed out. It is related to the bulk resistance of the organic semiconductor rather than any contact resistance, shows a weak temperature dependence, and is typically well described by empirical Lorentzian $\Delta R/R \propto B^2/(B^2 + B_0^2)^2$ or "non-Lorentzian" $\Delta R/R \propto B^2/(|B| + B_0)^2$ line shapes, where the line width parameter B_0 is a few mT.

Several models have been proposed to explain the effects. Common in the different proposed models is that the magnetic field reduces spin mixing of pairs of quasi-particles, thereby influencing their spin-dependent interaction.

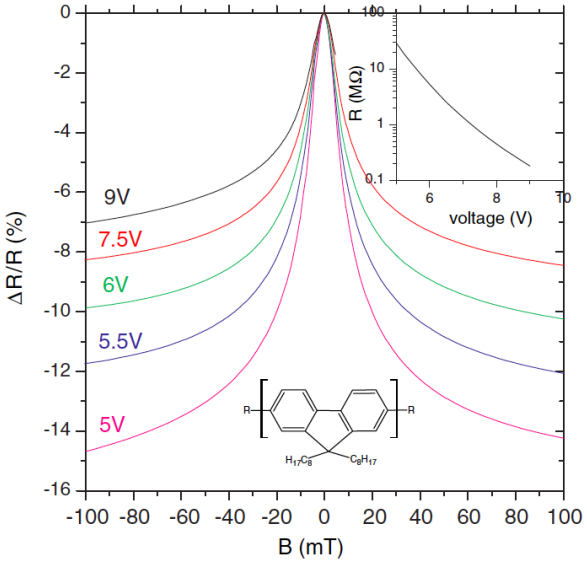

Figure 1: Room-temperature magnetoresistance in an ITO (30 nm)/PEDOT (≈100 nm)/PFO (≈100 nm)/Ca (≈50 nm including capping layer) device as a function of bias voltage. The device resistance versus applied voltage is shown in the inset. (After Ref. [23]).

Compelling evidence exists that the HFI is important for spin mixing. Clear differences could be observed in studies of magnetic field effects in deuterated versus non-deuterated organic semiconductors [28, 29]. Below we also discuss a recent report on direct electrical detection of nuclear spin manipulation in an OLED [30]. The mechanism at play is the following: Random precession of spins in the hyperfine fields introduces mixing between singlet and triplet character of spin pairs. This is suppressed by applying a sufficiently large magnetic field, such that the precession is no longer random. Mixing between singlet and triplet states no longer occurs, which impacts the interaction between the particles in the pair, ultimately resulting in a change in an observable such as the resistance or light output. Hyperfine fields in organic semiconductors are of the order of 1 mT, such that the fields required to affect spin-dependent interactions are small.

The different pairs of quasi-particles that have been considered to play a role (see Fig. 2) are polarons of equal charge forming bipolarons [31], polarons of opposite charge forming excitons [32], polarons and triplet excitons forming bound pairs [33], and triplet excitons that annihilate each other [34]. Recent studies show that a general explanation of the MR effect cannot be given based on a single mechanism. Rather, the dominating mechanism depends not only on the materials and device parameters, but also on operation conditions [35, 36].

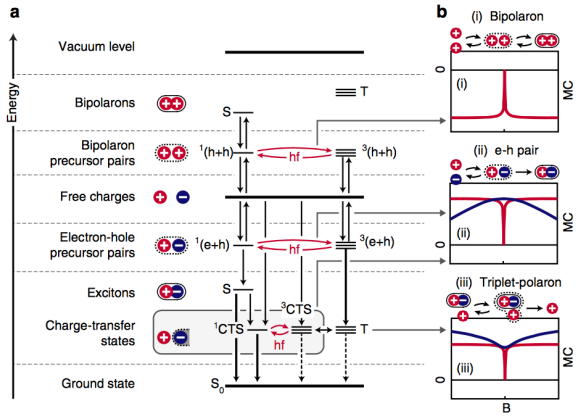

Figure 2: Overview of relevant particles and their spin-dependent reactions. (a) Possible quasi-particle pairs in organic semiconductors versus energy. Free charges may combine to form precursor pairs, either in a singlet $(S)^1()$ or triplet $(T)^3()$ configuration. Such a precursor pair can either recombine into an S or T exciton (for e-h pairs), an S bipolaron (for a bipolaron pair), a charge transfer state (CTS, for spatially separated e-h pairs), or dissociate into free carriers. Due to hyperfine fields (hf) the S and T configurations can mix (as indicated with curved arrows), while an external magnetic field suppresses this mixing. (b) The corresponding characteristic low (red) and high (blue) field line shapes according to a (i) bipolaron, (ii) e-h and (iii) triplet-polaron formation mechanism, all calculated using a density matrix formalism. (After Ref. [35]).

Direct probing of the coupling between charge-carrier spins and nuclear spins in an OLED has been carried out recently by Malissa et al., using pulsed electrically detected nuclear magnetic resonance spectroscopy [30]. This underlines the importance of hyperfine coupling for the magnetic field effects discussed previously. By studying devices containing deuterated or normal (hydrogenated) poly[2-methoxy-5-(2'-ethylhexyloxy)-1,4-phenylenevinylene] (MEH-PPV), signatures of deuterons and protons could be observed specifically in spin-echo envelope-modulation experiments. Detection of the effects relies on current measurement at constant bias voltage. Changes in the current are attributed to the changes in the recombination versus dissociation rates of bound polaron pairs of opposite charge.

A Hahn-echo technique is used (electron spin-echo envelope modulation, ESEEM), as in previously reported pulsed electrically detected magnetic resonance (EDMR) measurements on similar OLEDs, which demonstrated a spin dephasing time $T_2 \approx 350$ ns in MEH-PPV at room temperature [37]. Charge carrier spins are rotated by applying microwave pulses with a certain power and duration in a static magnetic field B_0 at the resonance frequency $g\mu_B B_0$, where g is the Landé g-factor and μ_B is the Bohr magneton. These effects are detected as a modulation of the Hahn-echo signal, which is measured electrically by recording current transients as a function of the delay time between microwave pulses. Fourier analysis of the signal versus delay time showed clear features (see Fig. 3) at 14.5 MHz for hydrogenated and at 2.2 MHz for deuterated MEH-PPV devices (the isotope specific signatures mentioned above).

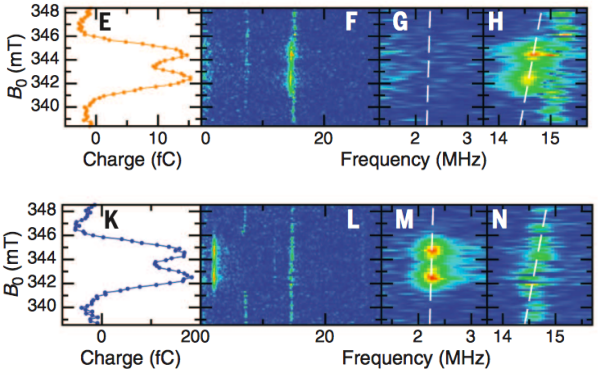

Figure 3: Magnetic field dependence (labeled E, K) and Fourier transforms (labeled F, L) of the ESEEM signal of hydrogenated (top) and deuterated (bottom) MEH-PPV, with zoomed in images for frequencies corresponding to deuteron (∼2 MHz, G,M) and proton (∼15 MHz, H, N) resonances. (After Ref. [30]).

Electrical detection of nuclear spin manipulation in this system was demonstrated at room temperature, using a "double-resonance scheme". This scheme involves radiofrequency (RF) pulses in addition to microwave pulses, to rotate nuclear spins. The effects of nuclear spin rotations on the populations of singlet and triplet polaron pairs were again detected by measuring current transients. This shows that it is possible to harness organic magnetic field effects for electrical readout of nuclear spin orientation.

A very appealing aspect of the effects described in this section is that they take place at room temperature, in weak magnetic fields. This is because they rely on changes in transition rate between states, rather than changes in the equilibrium occupations of states. Therefore, Zeeman splitting energies, which are orders of magnitude smaller than the thermal energy, are irrelevant. The magnetic field effects are thus kinetic in origin, and the models described above do not contradict equilibrium thermodynamics. It is worthwhile to point out that this is well understood in the spin-chemistry community, where spin-dependent chemical reactions between radical pairs are concerned.

The work of Malissa et al. illustrates that organic materials may be used in the near future for *room-temperature* quantum-coherent spin manipulation. In this context, a

truly fascinating analogy can be made with the quantum-biological compass that is believed to enable organisms such as migratory birds to sense the Earth's magnetic field [38, 39].

So far, the discussion has been limited to systems exhibiting equilibrium (i.e. zero) charge-carrier spin polarization. When out-of-equilibrium spin polarization is introduced, a plethora of additional effects comes into play, which we discuss in the following sections.

4 Organic spin valves and pseudo spin valves

4.1 Generic spin valves

Ferromagnetic materials, which feature a built-in spin polarization of their electronic structure, are ubiquitous in spintronics [1]. They form the basis of giant magnetoresistance (GMR) sensors and magnetic tunnel junctions (MTJs) [40], which are widely used in commercial technologies (hard disk read heads, sensors, memories) [41]. They are also widely used in the field of semiconductor spintronics [42, 43], e.g. to establish a non-equilibrium spin concentration in a non-magnetic semiconductor such as GaAs or Si via injection/extraction of spin-polarized charges or spin pumping.

It is a natural, interesting and rewarding avenue to explore whether the combination of ferromagnetic materials and organic materials may be used to develop spintronic devices. In this section, we will briefly review some important early works that have addressed this. Several recent studies will be highlighted as well.

A prototypical device that relies on spin-polarized currents is a "spin valve" [1]. The basic building blocks of a spin valve are two ferromagnetic electrodes separated by a spacer, which decouples them magnetically, but allows for an electrical current to flow. Spin-valve action is obtained if the current flow depends on the magnetization alignment of the ferromagnetic electrodes, such that e.g. a high resistance state is obtained for anti-parallel alignment (valve closed), and a low resistance state for parallel alignment (valve open). Examples of such devices are GMR sensors and MTJs.

In a pioneering study, Dediu et al. reported room-temperature magnetoresistance in devices comprising ferromagnetic $La_{0.7}Sr_{0.3}MnO_3$ (LSMO) electrodes and a sexithienyl (6T) spacer [44]. LSMO films were patterned into electrodes separated by a narrow gap (100–500 nm), which was filled by 6T to form lateral devices. The resistance of the devices showed a clear magnetic-field dependence. This work inspired the first experiments on organic spin valves, consisting of ferromagnetic LSMO and Co electrodes separated by an Alq_3 spacer (thickness 100–200 nm), in a vertical layer stack (layers deposited onto each other) [45]. Low- and high-resistance states were obtained for anti-parallel and parallel magnetization of the LSMO and Co contacts. The associated MR reached up to 40% at low temperature (about 10 K). The spin-valve effects could be observed up to 200 K, at low bias voltages (< 1 V). Similar experiments have been performed afterwards by many research groups, demonstrating spin-valve behavior in a large variety of systems containing different ferromagnetic electrodes and organic semiconductors [46, 47].

4.2 Organic spin valves operating in the tunneling regime

When the organic spacer layers are very thin (typically <10 nm), charge transport takes place via direct and/or multistep tunneling rather than thermally activated hopping. The device physics of organic spin valves with such very thin organic spacers is therefore quite similar to that of inorganic, e.g. metal/insulator/metal, magnetic tunnel junctions. For direct tunneling through an insulating (or semiconducting) barrier, the tunnel magnetoresistance (TMR) is determined by the tunnel spin polarization of both ferromagnetic contacts (P_1, P_2). The parameters P_1 and P_2 depend on the spin polarization of the interfacial DOS on either side of the barrier, and therefore on the electronic and magnetic properties of the ferromagnet/barrier interfaces. In addition, the (intrinsic properties of the) tunnel barrier may affect the tunnel spin polarization via different transmission probabilities for different states. The TMR is usually defined as $(R_{AP}\text{-}R_P)/R_P$ (multiplied by 100% when given as a percentage), where R_{AP} and R_P are the junction resistances for antiparallel and parallel magnetization of the electrodes. It can be related to the tunnel spin polarization according to the relation TMR = $2P_1P_2/(1\text{-}P_1P_2)$.

In 2003, it was shown that coherent spin transfer between quantum dots could be achieved by tunneling through conjugated spacer molecules [48]. This showed that it is conceptually possible to make spin valves with molecular tunnel barriers. Such devices were first demonstrated using nanopore contacting of octanethiol self-assembled monolayers on Ni [49]. Octanethiol molecules contain saturated, sp^3-hybridized carbon atoms and hence exhibit a wide band gap. For tunneling through barriers composed of such molecules, inelastic scattering due

to molecular vibrations has been proposed to play a role, based on measurements of the bias dependence of the magnetoresistance [50, 51]. Santos *et al*. reported magnetic tunnel junctions incorporating π-conjugated molecules, i.e. molecules with a much smaller band gap (see Fig. 4). The Co and $Ni_{80}Fe_{20}$ electrodes in these devices were separated by a composite barrier, AlO_x/Alq_3, with Alq_3 thickness between 1 and 4 nm [52]. Magnetoresistance values up to 6% at room temperature were observed. The resistance of the junctions was found to scale exponentially with Alq_3 thickness, consistent with tunneling through the Alq_3 barrier. In addition, however, the junction resistance showed quite a strong temperature dependence compared to that of magnetic tunnel junctions with inorganic insulating barriers: the resistance increased by a factor 2-3 upon cooling down from room temperature to 4.2 K. This shows that thermally activated processes are in play.

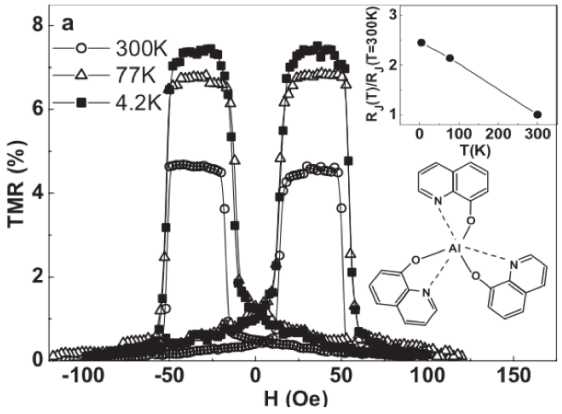

Figure 4: TMR measured with a 10 mV bias voltage of a junction consisting of Co(8 nm)/Al_2O_3(0.6 nm)/Alq_3(1.6 nm)/Permalloy (10 nm). The temperature dependence of the resistance is shown in the upper inset. The lower inset shows the chemical structure of the Alq_3 molecule. (After Ref. [47]).

Similar devices were studied by Schoonus et al. [53], with structure CoFeB/AlO_x/Alq_3/Co, where the thickness of the Alq_3 layers was again varied between 1 and 4 nm. MR values of a few percent were measured for the thickest Alq_3 layers at room temperature. The temperature dependence was not discussed in detail, but it was mentioned that a 60% increase of the resistance was observed upon cooling down from room temperature to 4.2 K. Using the dependence of the junction resistance on Alq_3 thickness, the authors identified a transition from direct tunneling through the composite AlO_x/Alq_3 barrier to multistep tunneling via intermediate states in the Alq_3 layer, which occurs as the Alq_3 thickness increases. At the onset of multistep tunneling, a reasonable description of the transport mechanism is a combination of direct tunneling and two-step tunneling, involving a single intermediate Alq_3-derived state. Using a model based on such a picture, the magnetoresistance could be calculated, yielding a reasonable description of the experimental results. The main effect of the involvement of this intermediate state in two-step tunneling processes is a strong reduction of the magnetoresistance, even if there is no spin relaxation in the intermediate state.

We reported similar phenomena in our own experiments and modeling of spin valves with structure $Co/AlO_x/C_{60}/Ni_{81}Fe_{19}$ comprising ultrathin C_{60} layers (several nm) [54]. For junctions with a C_{60} thickness below 10 nm, room-temperature MR of a few percent was observed. As for the study of Schoonus et al., the experimental results could be reasonably described using a multistep tunneling model (see Fig. 5). In the multistep tunneling regime, the MR is strongly attenuated and the junction resistance becomes increasingly temperature dependent. We based our model calculations on a superposition of direct and multistep tunneling, where the latter takes place via a Gaussian DOS of intermediate states in the C_{60} layer. This Gaussian DOS results from energetic disorder of LUMO-derived states. It was found that the magnetoresistance drops continuously as the amount of intermediate tunneling steps increases, irrespective of the spin lifetime and spin diffusion length in C_{60}. Consequently, these parameters cannot be extracted simply from the thickness dependence of the magnetoresistance, as has been common practice (see Refs. [46, 47] and the references therein).

In the multistep tunneling regime, the MR is of course also affected by spin relaxation that occurs as charge carriers occupy intermediate states in the organic spacer. This issue was already addressed for two-step tunneling processes by Schoonus et al., who considered spin precession due to random hyperfine fields [53]. Roundy et al. extended this concept to processes involving multiple intermediate states in the organic spacer [55, 56]. They suggested that a key role is played by quantum mechanical interference of spin rotation amplitudes during hopping in a random hyperfine field, which may lead to large spatial variations, and even sign reversal [56], of the magnetoresistance for different current paths.

Nanoscale organic spin valves operating in the (multistep) tunneling regime were reported by Barraud et al. [57]. LSMO/Alq_3/Co nanojunctions were fabricated using a nano-indentation scheme based on CP-AFM. Due to the small tip-radius of 10 nm, correspondingly small junction areas could be obtained. Indentation was carried out such that a few nm Alq_3 remained between bottom- and top contacts. Some of the junctions fabricated in this way

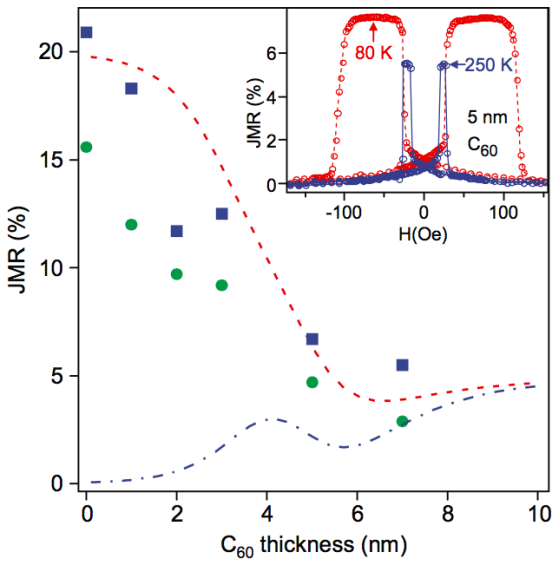

Figure 5: Junction magnetoresistance (JMR) as a function of C_{60} thickness for junctions consisting of Co(8 nm)/Al_2O_3(2 nm)/C_{60}(x nm)/$Ni_{81}Fe_{19}$(15 nm). The data points correspond to measurements performed at room temperature (solid circles) and 5 K (solid squares). Also shown are model calculations for a combination of direct and two-step tunneling (dashed line) and two-step tunneling only (dash-dotted line). The inset shows the resistance versus magnetic field of a junction with 5 nm C_{60} (plotted as a JMR value), measured at 250 K (blue) and 80 K (red). (After Ref. [49]).

showed very large MR at low temperature, up to 300% at 2 K. It was argued that the MR in organic spin valves is strongly influenced by resonant tunneling through interfacial states, i.e. states formed by hybridization of molecular orbitals with continuum bands of the ferromagnetic contacts (see also discussion below). In particular, it was argued that the different behavior of these nanoscale junctions as compared to their large area counterparts (typically hundreds of μm^2 or larger) might be attributed to spatial and energetic disorder of interfacial states. The large positive MR (defined as $(R_{AP}\text{-}R_P)/R_P$) of the nanoscale junctions as compared to the generally negative MR observed in "large area" junctions might then be explained by a different sampling of the distribution of such states. As pointed out by Roundy et al. [56], however, other effects not related to interfacial properties might also play a role in the multistep tunneling regime.

4.3 Organic spin valves with "thick" organic spacers

Following the seminal work of Xiong et al. [45], many experimental studies have been devoted to organic spin valves with relatively thick organic spacer layers, on the order of 100 nm. This is clearly too thick to allow for carriers to tunnel through, and charge transport is expected to be dominated by thermally activated hopping in the organic semiconductor. Consequently, spin-valve behavior should result from the transport of spin-polarized carriers through the organic spacer, and different transmission rates for spin-up/spin-down carriers at the organic/ferromagnetic interfaces.

However, magnetoresistance is typically observed in devices that exhibit only a modest temperature dependence of the resistance [45], which is at odds with a picture of thermally activated hopping and points to (direct or multi-step) tunneling-based conduction instead. For some systems, MR is observed in the tunneling regime while it is absent in the thermally activated transport regime [58], supporting the view that MR in organic spin valves may generally be associated with tunneling effects. On the other hand, other systems have been reported that *do* exhibit significant MR in combination with a strong temperature dependence of the conductivity [59, 60]. In addition, strong isotope effects have been reported in organic spin valves based on deuterated and hydrogenated versions of the same conjugated polymer [28], supporting the idea that spin-polarized transport in the organic layer plays a dominant role. At present, the debate about the origin of MR in these devices is far from settled (see also discussion further below).

As was recognized early on, a problem related to the tunneling-like characteristics is conduction via defects. Defects can include pinholes in the organic layer or metallic filaments, which could possibly be at the origin of some of the MR effects observed in organic spin valves. Such defects are difficult to detect, and therefore very difficult to exclude, especially in large-area devices. The top organic-semiconductor/ferromagnetic-electrode interface in the layer stack is a potential source for such problems, since it is typically formed by using metallic vapor to deposit a metal layer onto the organic film. Diffusion of metal atoms into the organic film may then assist the formation of metallic filaments. Such diffusion effects are well known in the organic electronics community, and have been addressed as well in the context of organic spintronic devices [61–64].

Considerable effort has been devoted to the fabrication and characterization of organic spin valves with improved interfacial properties, i.e. devices in which interdiffusion at the organic-semiconductor/ferromagnetic-contact interface is minimized. One possible route is the incorporation of insulating barrier layers at that interface. For example, in case of LSMO/Alq_3/Co spin valves, adding

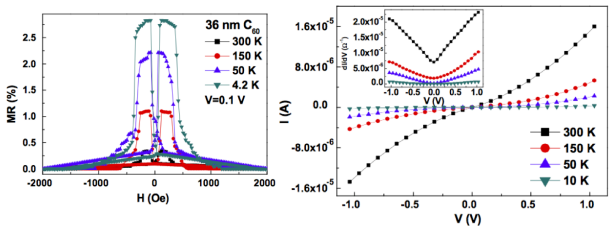

Figure 6: Temperature dependent MR (left) and IV characteristics (right) of LSMO/C_{60} (36 nm)/AlO_x(1. nm)/Co spin valves. (After Ref. [55]).

an AlO_x barrier layer between Alq_3 (100–300 nm thick) and Co resulted in devices with improved characteristics, exhibiting room-temperature MR of about 0.1% [65]. A recent report on LSMO/C_{60}/AlO_x(1.5 nm)/Co spin valves showed large room- temperature MR of about 2.5% for junctions with 36 nm C_{60} layers (see Fig. 6), for which the temperature dependence of the conductivity σ could be fitted by the relation $\sigma = \sigma_o \exp(-T_o/T)^{1/4}$, consistent with thermally activated hopping [60]. Another approach is buffer-layer-assisted growth, where an inert Xe layer is first condensed onto the organic semiconductor at low temperature, and ferromagnetic clusters are then deposited on top. Upon desorption of the Xe layer by annealing, the clusters land on the organic substrate. By repeating this process several times, a continuous ferromagnetic contact can be obtained. Large MR up to about 300% at 10 K has been observed in LSMO/ALq_3/Co spin valves fabricated in this fashion [66].

The ferromagnetic/organic interfaces in organic spin valves are generally not engineered for obtaining low charge-injection barriers. Ferromagnetic metallic contacts that exhibit a robust spin polarization of electronic states near the Fermi level are required. This strongly limits the freedom for tuning injection barrier heights. A recent study on Co/AlO_x/bathocuproine(BCP)/$Ni_{80}Fe_{20}$spin valves [59], where the properties of the AlO_x barriers were varied and different barrier heights were found, suggests that this might nevertheless be of considerable importance. For a BCP thickness up to 60 nm, room-temperature MR of a few percent, in combination with a strongly temperature dependent conductivity consistent with thermally activated hopping, was observed for devices with low injection-barrier heights (determined from $\ln(I/V^2)$ versus V^{-1} plots) at the Co/AlO_x/BCP interface.

It is worth pointing out that in some cases organic spin valves exhibit additional characteristics (other than magnetoresistance) that could potentially be exploited. A salient example is the occurrence of memristive effects in LSMO/Alq_3/Co spin valves [67]. These effects have been ascribed to filamentary conduction, involving voltage-driven formation of highly conductive filaments connecting the electrodes. The coupling between memristor- and spin-valve action in a single device is very interesting, and may lead to new types of applications.

4.4 Tunneling anisotropic magnetoresistance in pseudo spin valves

The spin orbit coupling (SOC) in crystalline solids is anisotropic, since it originates from the electric fields resulting from the nuclei and electrons forming the crystalline lattice. Due to this anisotropy of the SOC in ferromagnetic crystals, the spin-dependent DOS is modulated as the magnetization direction (and therefore the spin quantization axis) is varied along different crystallographic directions [68]. This effect lies at the origin of magnetocrystalline anisotropy and anisotropic magnetoresistance in ferromagnetic metals. In magnetic tunnel junctions, it may give rise to a resistance change upon changing the magnetization direction of the ferromagnetic electrodes. This effect, called tunneling anisotropic magnetoresistance (TAMR), was first reported for devices that contained only a single ferromagnetic (Ga,Mn). As contact, an AlO_x tunnel barrier, and a nonmagnetic Ti/Au counter-electrode [69]. It was also recently found in devices based on organic semiconductors.

Gruenewald et al. demonstrated spin-valve-like MR in structures comprising a ferromagnetic LSMO electrode, a perylene diimide derivative (PTCDI-C4F7) as organic spacer, and a nonmagnetic Al contact [70] The hysteretic behavior of the MR followed the two-level switching of the LSMO electrode, and could be attributed to TAMR originating from that electrode. We recently reported strong TAMR effects in Co/AlO_x/C_{60}/Al junctions (see Fig. 7) [71]. The effect originates from the anisotropic SOC in the Co electrode, which is grown epitaxially on a sapphire (0001) substrate, with fcc (111) out-of-plane orientation and in-plane epitaxial relations Co $(111)[1\text{–}10]_{fcc}||Al_2O_3$ $(0001)[1\text{–}100]$ and Co $(111)[\text{–}110]_{fcc}||Al_2O_3$ $(0001)[\text{–}1100]$. In Co/AlO_x/Al tunnel junctions without C_{60} interlayer, the in-plane and out-of-plane TAMR values at 5 K are 7.5% and 11%, respectively [72]. The magnitude of the effect is reduced in Co/AlO_x/C_{60}/Al junctions, but it persists in the multi-step tunneling regime. The in-plane TAMR effects are on the order of 1% at 5 K and low bias for 8 nm C_{60} interlayers in Co/AlO_x/C_{60}/Al junctions [71].

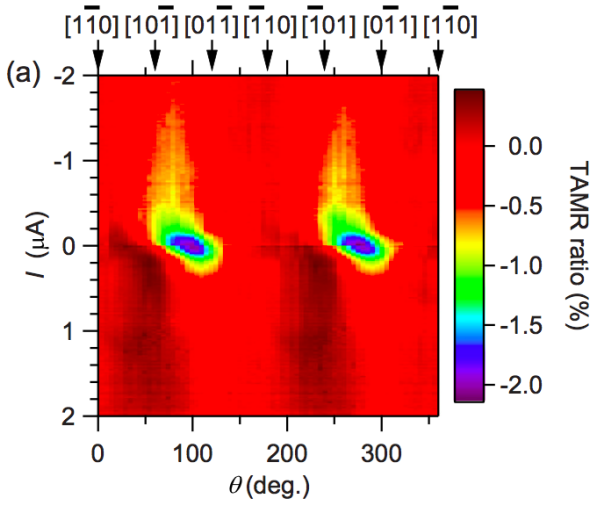

Figure 7: TAMR (in percent, color scale), versus in-plane magnetization angle and bias current, of a junction consisting of Co(8 nm)/AlO_x(3.3 nm)/C_{60}(4 nm)/Al(35 nm), measured at 5 K. A magnetic field of 500 mT was used to saturate the in-plane magnetization of the fcc-Co (111) electrode along different in-plane directions, various crystallographic directions are indicated. For this particular C_{60} thickness, a TAMR effect of up to ∼2% is observed (After Ref. [71]).

4.5 Organic spin valves: where are the carrier spins?

From the above, it should be clear that the device physics of organic spin valves is far from understood, in spite of the various models proposed to explain their operation [53, 54, 57, 73–75] Perhaps the most fundamental question that still needs answering is whether the observed magnetoresistance effects are in any way related to the injection, transport and extraction of spin-polarized carriers in/from the organic semiconductor spacers, instead of, or in addition to, tunneling effects. While muon spin rotation measurements [76] and two-photon emission experiments [77] suggest that it is in principle feasible to obtain charge carrier spin polarization in an organic semiconductor using a ferromagnetic contact, these studies do not provide any information on the relation between such spin polarization and MR in organic spin valves.

Spin precession phenomena, akin to those giving rise to the magnetic field effects discussed in section 3, could shed light on this issue. Measurements of Hanle precession of spins in a magnetic field that is non-collinear with the spin quantization axis can provide unambiguous proof of spin injection in nonmagnetic materials, as has been demonstrated for inorganic semiconductors [78, 79], metals [80, 81], and superconductors [82]. The method is not specific for any particular materials system, and should be applicable to organic semiconductors. Several groups have investigated the behavior of organic spin valves in magnetic fields that were perpendicular to the in-plane magnetization of the ferromagnetic electrodes, such that Hanle precession of spins injected into the organic spacer should occur. The Hanle precession of an electron in a magnetic field perpendicular to its spin proceeds with the Larmor frequency ω_L given by $\omega_L = egB/(2m_e)$, where e is the unit charge, g is the Landé g-factor, B is the magnetic field, and m_e is the electron mass. The precession changes the orientation of the spin during transit in the organic spacer. If the MR effect is indeed related to spin injection and transport, it should depend on the relative orientations of (1) the magnetization of the two first electrodes, (2) the spins of the charge carriers traversing through the organic layer, and (3) the magnetization of the second electrode. Therefore, the resistance of the device should change if spin precession occurs during transit.

Riminucci et al. studied LSMO/Alq_3/AlO_x/Co spin valves with 200 nm Alq_3 layers, and found no Hanle effect [83]. This finding could only be reconciled with spin-polarized transport if the carrier mobility was exceptionally high (resulting in a small precession angle during transit), i.e. larger than 30 $cm^2 V^{-1} s^{-1}$. This is much larger than the intrinsic electron mobility in Alq_3. The authors proposed that transport in their devices might occur via highly conductive filaments. As mentioned above, a similar picture has been invoked to explain memristor behavior in these spin valves [67]. Gruenewald et al. investigated organic spin valves with Alq_3 (40–100 nm) and PTCDI-C4F7 (100–600 nm) spacers, and LSMO (bottom) and CoFe (top) electrodes [84]. Again, no Hanle effect could be observed. The MR observed in these devices was attributed to (multi-step) tunneling via pinholes in the organic layers in combination with TAMR originating from charge injection at the LSMO/organic interface. The latter could be demonstrated by studying the resistance of the devices as a function of the in-plane magnetic field direction with respect to the crystalline axes of the LSMO electrode.

It should be pointed out that even though the observation of a Hanle effect would be unambiguous proof for spin injection, its absence does not necessarily rule out that any spin injection takes place. It has been suggested that the magnetic fields needed to observe a Hanle effect in organic semiconductors might be much larger than previously thought, due to an exchange-induced spin-transport mechanism between localized charges that does not require slow hopping of these charges [85]. Nevertheless, unless unambiguous proof for spin injection is found, by Hanle measurements or otherwise, it is not possible to conclusively ascribe MR effects in organic spin valves to spin-

polarized charge transport through the organic semiconductors.

5 Spin pumping in organic semiconductors

The devices discussed in the previous section all operate via spin-polarized charge currents. This leads to charge accumulation, in addition to spin accumulation, which considerably complicates the physics. We now discuss a method that avoids the generation of charge accumulation. Pure spin currents (without any accompanying charge current) can be generated in non-magnetic materials using "spin pumping", which is the inverse effect of spin-current- induced magnetization reversal, commonly referred to as spin-transfer torque. In ferromagnetic/non-magnetic heterostructures, forced precession of the magnetization vector of the ferromagnet acts as a spin pump, transferring angular momentum into the non-magnetic material in the form of a pure spin-current [86]. Recently, Watanabe et al. used this concept to generate a pure spin current in a π-conjugated polymer [87]. A three-layer sandwich device structure was used, comprising a $Ni_{80}Fe_{20}$ ferromagnetic layer, a thin film of poly(2,5-bis(3-alkylthiophen-2-yl)thieno[3,2-*b*]thiophene) (in short PBTTT), and a Pt electrode. Using a ferromagnetic resonance (FMR) technique, the magnetization of the $Ni_{80}Fe_{20}$ layer was made to precess, resulting in a spin current injected into the PBTTT film. The spin current arriving at the PBTTT/Pt interface was detected using the inverse-spin Hall effect (ISHE), which generates a transverse voltage across the Pt electrode. A clear ISHE voltage signal, V_{ISHE}, could be detected upon sweeping an (in-plane) external magnetic field through the resonance condition, under application of a constant microwave excitation (see Fig. 8). The signal was found to scale with the spin Hall angle (originating from SOC) of the non-magnetic electrode material used. Replacing Pt by Au reduced the ISHE voltage by about a factor of 30, while it could no longer be detected with a Cu electrode. The spin current was proposed to be carried by polarons in the PBTTT, which could result from unintentional doping and/or thermal injection from the contacts. (The estimated residual charge carrier concentration in the PBTTT was about $2\times10^{15}cm^{-3}$, based on capacitance-voltage measurements). A control experiment using a device containing an insulating polymeric interlayer did not show any ISHE signal, which is consistent with this. Upon tilting the FMR magnetic field out-of-plane, the variation of the V_{ISHE} with the out-of-plane angle θ was found to be consistent with Hanle precession of spins in the PBTTT layer.

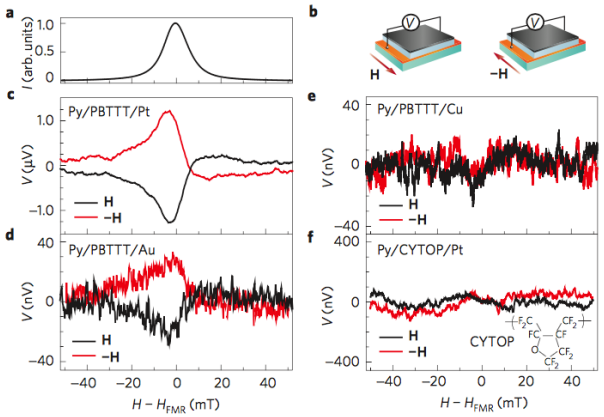

Figure 8: Spin pumping experiments in PBTTT. (a) Magnetic field (H) dependence of the FMR signal (microwave absorption intensity I) measured for a $Ni_{80}Fe_{20}$(10 nm)/PBTTT(40 nm)/Pt(7 nm) junction, at 100 mW microwave excitation. The external magnetic field was applied along the film plane, as shown in (b). VISHE measurements as a function of magnetic field (under 100 mW microwave excitation) are shown for different junctions: (c) $Ni_{80}Fe_{20}$(10 nm)/PBTTT(40 nm)/Pt(7 nm), (d) $Ni_{80}Fe_{20}$(10 nm)/PBTTT(40 nm)/Au(40 nm), (e) $Ni_{80}Fe_{20}$(10 nm)/PBTTT(40 nm)/Cu(300 nm), and (f) Ni80Fe20(10 nm)/CYTOP(60 nm)/Pt(7 nm). The chemical structure of the insulating CYTOP is shown in the inset of (f). Black and red lines correspond to experimental data recorded with the in-plane fields H and –H, respectively (After Ref. [87]).

The V_{ISHE} measurements were found to be weakly dependent on temperature in the temperature range studied, between 200 and 300 K. Because of this, the authors proposed that the main spin-relaxation mechanism at play was SOC-induced spin flipping during hopping events. In such a picture, a longer spin lifetime is expected at low temperature, resulting in correspondingly low hopping rates. The spin lifetime is then inversely proportional to the carrier mobility, such that the spin diffusion length becomes largely temperature independent. It should be pointed out, however, that the experiments were performed under application of relatively large magnetic fields (on the order of 100 mT) to achieve spin pumping, such that spin relaxation due to random hyperfine fields is suppressed. The results therefore do not allow for conclusions to be drawn regarding spin relaxation in weak (or zero) magnetic fields.

The use of a pure spin current in the spin-pumping experiment eliminates difficulties related to the creation of carrier spin polarization via the injection of charge currents, as is the case for organic spin valves. Therefore, the

scheme is an attractive alternative for studying spin transport in organic semiconductors. In spite of the promising results, there are also some problems that warrant further investigation. The results suggest an anomalously large spin current, which perhaps could be reconciled with a mechanism of exchange-mediated spin transport [77], in contrast to slow polaron hopping.

6 Spin dependent effects at hybrid interfaces

In previous sections, the importance of orbital hybridization at ferromagnet/organic interfaces for spintronic devices has already been mentioned. We now explicitly discuss these effects. When organic semiconductors are deposited onto ferromagnetic surfaces, mixing of molecular orbitals and the spin-split valence electronic states of the ferromagnet typically results in hybrid orbitals that are spin polarized. Spin-dependent orbital hybridization may be used to make interfaces with a particular magnetic and electronic structure, which in turn may be used for spintronic devices. This approach, which has been coined "spinterface science" [57, 88], has become a very active field of research. It has been shown that, due to orbital hybridization, the spin polarization at ferromagnetic surfaces may be amplified or inverted [57, 89], spin-filtering tunneling may occur at molecular adsorbate sites [90], and non-magnetic metallic layers may even become ferromagnetic upon interface formation with carbon-based molecules [91]. In addition, interfacial magnetoresistance due to a single ferromagnetic/molecular interface has been demonstrated [92]. These effects will be discussed in some detail below.

The 3d transition metals, Fe, Co, and Ni are archetypical FM electrode materials. They exhibit a modest spin polarization compared to, for example, half-metallic Heusler alloys or manganites, but offer clear technological advantages. The partly filled 3d orbitals of Fe, Co, and Ni lead to rich surface chemistry with molecular adsorbates, which is exploited in a plethora of catalytic reactions. Such surface chemistry might also be used to tailor the surface magnetic and electronic structure of 3d transition metal ferromagnets. This has been studied in some detail for various π-conjugated molecules adsorbed on ferromagnetic surfaces. The most common experimental techniques to probe the interface electronic and magnetic structure are x-ray magnetic circular dichroism (XMCD) [93–95], spin-polarized scanning tunneling microscopy (SP-STM) [90, 96–98], spin-polarized metastable de-excitation spectroscopy(SP-MDS) [99–101], spin-polarized ultraviolet photoelectron spectroscopy (SP_UPS) [102–104], and spin-resolved two-photon photoemission (SR-2PPE) [77]. Modeling is typically done with density functional theory (DFT) [89, 95, 97, 98, 104–109].

In a substantial number of studies, the interactions between ferromagnetic metal surfaces and aromatic (i.e. with a flat ring structure) π-conjugated molecules have been studied. In particular, metal-phthalocyanines (Pc's) and porphyrins have received a considerable amount of attention [89, 93, 96, 97, 99, 103–105, 107]. The metal ions in these metallo-organic molecules typically have unpaired spins, which are found to couple to the ferromagnetic substrate via the exchange interaction. The presence of such ions allows for element specific magnetic probing with XMCD [93]. This technique relies on the excitation of core-level electrons with circularly polarized x-rays into unoccupied states to probe the magnetic polarization of the conduction band. For 3*d* transition metal ions, *L*-edge XMCD spectra provide quantitative information on the magnetic spin and orbital moments, which can be applied to the orbitals involving the central metal ions in metal-Pc's and porphyrins.

Brede *et al.* studied CoPc molecules on ∼1.8 Fe ML on W(110) with SP-STM and DFT calculations (see Fig. 9) [97]. SP-STM probing of CoPc molecules was performed on the two-layer portion of the Fe film, which grows pseudomorphically on W in a layer-by-layer fashion, despite the significant lattice mismatch. On W(110), the Fe(110) layers are ferromagnetic from the first (sub)monolayer [110]. While electron transfer from the substrate to the CoPc molecule eliminates the unpaired spin, orbital hybridization leads to spin-split interfacial states. Depending on the exact location on the molecule and the energy region that is sampled, the spin polarization is reduced, enhanced or inverted as compared to the bare surface. These effects are due to the hybridization of different molecular orbitals, localized on different segments of the molecule and residing at different binding energy, with the spin-split *d*-bands of the Fe surface. Note that a recent study of spin-transport devices incorporating CoPc layers also shows the importance of ferromagnet/molecular orbital hybridization, e.g. giving rise to the new additional feature of large range control of the coercive field by the electric field [111].

Qualitatively similar behavior was found in theoretical studies of a series of small aromatic molecules [89], namely benzene, cyclopentadienyl radical, and cyclooctatetraene adsorbed on the same substrate, ∼2 monolayers of Fe on W(110). These molecules exhibit different electronegativity and reactivity, such that the strength of the interaction with the Fe surface is different. For

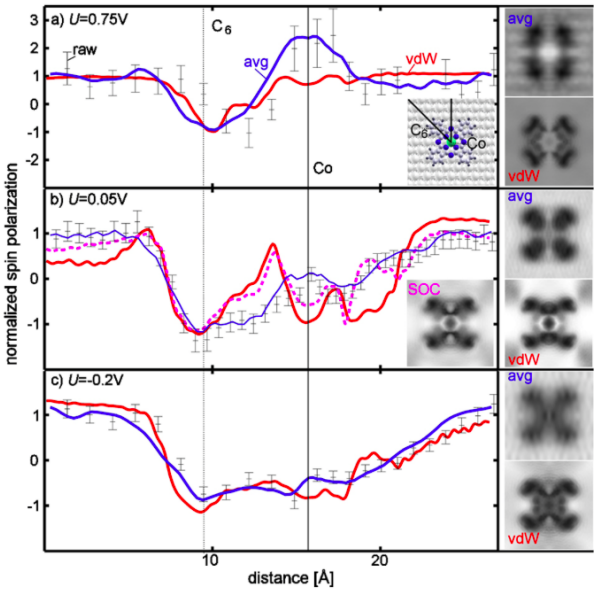

Figure 9: Local spin polarization, as probed by SP-STM, of a CoPc molecule on ∼1.8 Fe ML on W(110), for three different energies. Raw data and averages (over multiple images, blue lines) are compared with DFT simulations including van der Waals interactions (vdW, red lines) and spin-orbit coupling (SOC, pink dotted line in (b)). The line profiles are measured along high-symmetry directions, as indicated in the sphere model inset in (a). Simulated data including SOC are only given in (b), as the SOC corrections for (a) and (c) are negligible. The insets show measured and simulated SP-STM images of 2.2 × 2.2 nm. (After Ref. [89]).

these molecules, attenuation and inversion of the surface spin polarization was found, again dependent on the exact location and sampled energy window. Stronger inversion was obtained with increasing interaction strength, which is relatively weak for benzene, and strong for cyclopentadienyl radical and cyclo-octatetraene. This shows that it is possible to engineer the spin polarization via the molecule-substrate interaction. Additional support for this was provided in theoretical work on benzene and cyclopentadienyl radical adsorbates with varying electronegativity, due to substitution of hydrogen atoms with more electronegative chlorine and fluorine atoms [106]. The magnetic moment residing on the molecule was found to scale with the electronegativity.

Our own studies of C_{60} molecules adsorbed on ultrathin Fe(100) films (grown epitaxially onto MgO (100) single crystalline substrates) also show a significant effect of orbital hybridization on the magnetic structure of the interface [94, 95]. In contrast to the case of flat, aromatic molecules, only a limited fraction of the carbon atoms bond directly to substrate atoms. Nevertheless, the frontier π and π^* orbitals, which are delocalized over the whole molecule, are significantly affected. The effects of hybridization are evident in C K-edge x-ray absorption spectroscopy (XAS) spectra of C_{60} monolayers adsorbed on Fe(100), showing broadening and shifts of peaks associated to different unoccupied molecular orbitals. The magnetic moment residing on the molecules due to mixing between C_{60} orbitals and Fe 3d wave functions was probed by XMCD. By measuring XAS spectra with opposite alignment of the photon helicity and (in-plane) substrate magnetization, a dichroic signal of about 3% of the maximum XAS intensity at the C K-edge of the C_{60}/Fe(100) interface was found. Such a robust XMCD signal indicates a sizeable magnetic moment on the C_{60}-derived orbitals. Due to the lack of spin-orbit coupling in the 1*s* ground state, K-edge dichroism probes the orbital moment in the π^*-band rather than the spin moment. Since the π^*-band is nearly filled, however, the spin moment is parallel to the probed orbital moment according to Hund's rules.

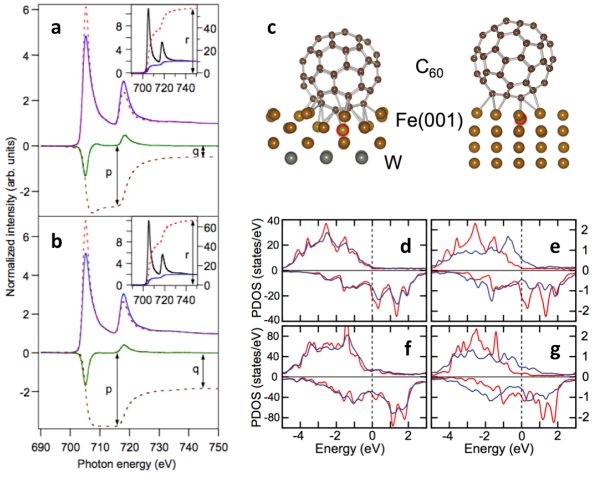

Figure 10: Electronic and magnetic structure of C_{60} on ∼3 MLs Fe on W(001). On the left: normalized XAS spectra recorded at opposite remanent magnetization (red and blue) and the corresponding XMCD spectra (green) plus integrated XMCD intensity (brown) measured at the Fe L2,3 edges, of (a) 3MLs of Fe on W(001) and (b) the same sample after deposition of several nm of C_{60}. The insets show the summed XAS spectra and their integrals; a stepped background (blue) was subtracted from the summed XAS spectra prior to integration. The adsorption geometry of the C_{60} molecule is depicted in (c), where the most significantly affected Fe atom is encircled in red. (d-g) DFT calculations of the projected DOS (PDOS) of majority (top) and minority (bottom) spin states, projected on the top Fe layer, are shown at (d) the C_{60}/Fe(001) interface (blue), compared to the PDOS of a clean Fe(001) surface layer (red). (e) shows the PDOS of the most strongly affected Fe atom (blue), compared to the PDOS of a clean Fe(001) surface atom; (f,g) as (d,e), but for the Fe/W(001) substrate. (After Ref. [87]).

As the excitation energy is varied, and hence different orbitals are probed, an inversion of the magnetic po-

larization of the C_{60} molecules relative to the magnetization of the Fe substrate can be observed from the change in sign of the XMCD signal. The LUMO-related moment is found to be opposite to the Fe-magnetization. This is consistent with DFT calculations, which show a magnetic moment of $\mu_S = -0.21\ \mu_B$ per molecule for C_{60} on Fe(001). We also studied the adsorption of C_{60} molecules on ultrathin Fe layers (∼3 monolayers, ML) grown pseudomorphically on W(001) [95]. This enables XAS/XMCD studies of the effect of orbital hybridization on the Fe-moments, which is hampered in thicker films by the significant contribution of the Fe bulk substrate to the XAS yield. In contrast to Fe on W(110), a single Fe ML orders antiferromagnetically on W(001) [112], while two or more ML are ferromagnetic with in-plane anisotropy. The calculated magnetic moment on C_{60} molecules adsorbed on ∼3 ML Fe on W(001) is similar to the case of C_{60} on "bulk" Fe(001), 0.27 μ_B per molecule. The magnetic moment of the surface Fe atoms is reduced due to the hybridization. XMCD experiments show a reduction of ∼6% of the Fe spin moment, which agrees well with averaged computational results (see Fig. 10). The latter show, however, that the hybridization-induced changes are rather inhomogeneous. Fe atoms that are directly involved in bonding to C_{60} molecules are most strongly affected, and have their moments reduced with up to 40%.

Many other interesting effects have been observed for systems involving C_{60}/transition-metal interfaces. For example, it has been shown that the magnetic properties of Co thin films, such as saturation magnetization, coercivity, and magnetic anisotropy, are strongly affected by interface formation with C_{60} molecules [113, 114]. Kawahara et al. performed ST-SPM measurements on C_{60} molecules adsorbed on magnetic Cr(001), showing that spin-split hybrid orbitals are formed [90]. Similar to the case of flat, aromatic molecules [89, 97], the spin polarization of the DOS at the molecular sites was found to be strongly dependent on position and energy with respect to the Fermi level, and amplification as well as inversion of the DOS as compared to the Cr surface was observed.

Very recently, it was demonstrated that even for non-magnetic metals, Cu and Mn, magnetism may emerge due to interfaces with C_{60} molecules [91]. Magnetic hysteresis was observed at room temperature in C_{60}/Cu and C_{60}/Mn stacks using magnetometry. In control samples containing thin Al or Al_2O_3 spacers between the C_{60} and Cu or Mn films, no magnetism was observed, confirming that the magnetic state arises from the interfaces. Increasing the Cu or Mn thickness also leads to quenching of the magnetization. In particular for C_{60}/Cu stacks, the magnetization depends very critically on the Cu thickness, with a maximum at 2.5 nm Cu, and a complete quenching above 4 nm. Low energy muon spin spectroscopy measurements, providing depth-dependent magnetic information, showed that the magnetic moments reside on the Cu layer in a thin film stack containing a 2.5 nm Cu film sandwiched between C_{60} layers. This fascinating study shows that hybrid interfaces between molecular materials and metals can produce new magnetic metamaterials, going far beyond tailoring of the magnetic structure of intrinsically magnetic surfaces.

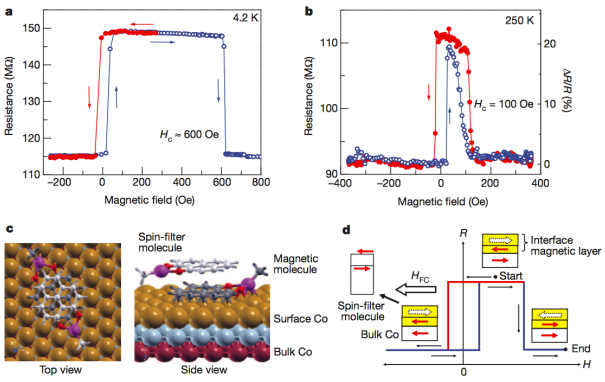

Figure 11: Interfacial magnetoresistance effects for ZMP adsorbed on Co. (a, b) MR measurements recorded with a sweeping magnetic field, for a junction consisting of Co(8 nm)/ZMP(35 nm)/ Permalloy(12 nm), (a) at 4.2 K showing a large switching field (∼600 Oe) attributed to the interface layer, and (b) at 250 K, showing large MR of 22% and a reduced switching field (∼100 Oe). (c) Adsorption geometry resulting from ab initio modeling: top view (left) and side view (right) of the relaxed adsorption configuration on a Co(111) surface (grey=carbon, red=oxygen, purple=zinc). The ZMP molecule in direct contact with Co ('magnetic molecule') absorbs flat on the Co surface and hybridizes strongly. The second molecule ('spin filter molecule') sits in a staggered configuration over the first, forming a molecular π-dimer. (d) Resistance R versus magnetic field H according to the device model, which considers an interfacial magnetic layer, consisting of the surface Co atoms hybridized with the molecular dimer. The relative magnetization directions are shown, of the interfacial magnetic layer and the bulk Co layer, at various field values (the arrow labeled HFC shows the direction of field cooling). The arrows in the schematic of the "spin-filter molecule" represent the spins of the LUMO-derived spin-split energy levels. (After Ref. [84]).

Magnetically ordered interfacial states at metal/molecular interfaces may give rise to remarkable magnetoresistance effects in devices, as was demonstrated by Raman *et al.* [92]. They showed large magnetoresistance effects (more than 20%) near room temperature in junctions containing interfaces between Co electrodes and zinc methyl phenalenyl (ZMP) molecules (see Fig. 11). These effects were observed in junctions containing both magnetic permalloy and non-magnetic Cu counter electrodes. Upon inclusion of an AlO_x spacer at the Co/ZMP interface, the effect disappeared, demonstrating its in-

terfacial origin (a small signal due to the ZMP/permalloy interface remained). The magnetic hysteresis of the resistance showed switching at the coercive field of the Co electrode, and another switch at significantly higher magnetic field attributed to magnetization reversal of the interfacial layer. The results were explained in terms of orbital hybridization between an adsorbed ZMP dimer and the Co substrate, modeled by DFT calculations. The two molecules making up the dimer interact differently with the ferromagnetic substrate: the molecule that is in direct contact with the surface Co atoms hybridizes strongly, whereas the orbitals of the second, largely decoupled molecule, are only weakly perturbed. This gives rise to a particular electronic and magnetic structure, where spin-filtering properties are assigned to the weakly interacting molecule. It exhibits small spin-splitting of its frontier π- and π^*-orbitals, giving rise to spin-dependent transmission of electrons originating from the interfacial layer. The latter consists of a magnetically hard (with respect to the bulk Co layer) hybrid ZMP/Co system. The magnetic hysteresis of the resistance is explained in terms of "independent" switching of the bulk Co film and the interfacial layer, enabled by the strongly reduced exchange integral at the Co surface (due to the reduced moment and number of neighbor atoms) and the magnetic anisotropy energy enhancement due to orbital hybridization.

7 Concluding remarks

Organic spintronics is a rich research field that continues to develop at a rapid pace. Spin-dependent recombination rates of various quasi-particles in organic semiconductors give rise to many magnetic field effects on observables as electrical resistance or light output of devices. These effects, which are largely analogous to spin-dependent chemical reactions studied in spin chemistry, do not require any out-of-equilibrium spin polarization and are intrinsic to the organic materials. Organic materials have been also successfully incorporated into hybrid inorganic/organic spintronic devices, where they may play a somewhat passive role as spacer between ferromagnetic electrodes, or a more active role by creating, via orbital hybridization, unique magnetic properties upon interface formation with electrode materials. Although a growing number of studies have revealed enormous technological potential, many of the effects are still quite poorly understood, which sets a challenging but also often rewarding task for the scientific community. A multidisciplinary approach, drawing knowledge from (theoretical and experimental) solid state physics and magnetism, device physics, (spin) chemistry, and surface science, seems most appropriate to face the many challenges that lie ahead in unlocking the potential of the field, and to unveil its many mysteries.

References

[1] Zutic, I., Fabian, J., Das Sarma, S., Spintronics: Fundamentals and applications, Rev. Mod. Phys., 2004, 76, 323-410.

[2] Kelley, T. W., Baude, P. F., Gerlach, C., Ender, D. E., Muyres, D., Haase M. A., et al., Recent progress in organic electronics: Materials, devices, and processes, Chem. Mater., 2004, 16, 4413-4422.

[3] Yu, Z. G., Spin-Orbit Coupling, Spin Relaxation, and Spin Diffusion in Organic Solids, Phys. Rev. Lett., 2011, 106, 106602.

[4] Yu, Z. G., Spin-orbit coupling and its effects in organic solids. Physical Review B, 2012, 85, 115201.

[5] Nuccio, L., Willis, M., Schulz, L., Fratini, S., Messina, F., D'Amico, M., et al., Importance of Spin-Orbit Interaction for the Electron Spin Relaxation in Organic Semiconductors, Phys. Rev. Lett., 2013, 110, 216602.

[6] Alam, K. M., Bodepudi, S. C., Starko-Bowes, R., Pramanik, S., Suppression of spin relaxation in rubrene nanowire spin valves, Appl. Phys. Lett., 2012, 101, 192403.

[7] Sheng, Y., Nguyen, T. D., Veeraraghavan, G., Mermer, O., Wohlgenannt, M., Effect of spin-orbit coupling on magnetoresistance in organic semiconductors, Phys. Rev. B, 2007, 75, 035202.

[8] Beljonne, D., Shuai, Z., Pourtois, G., Bredas, J. L., Spin-orbit coupling and intersystem crossing in conjugated polymers: A configuration interaction description, J. Phys. Chem. A, 2001, 105, 3899-3907.

[9] Pedash, Y. F., Prezhdo, O. V., Kotelevskiy, S. I., Prezhdo, V. V., Spin-orbit coupling and luminescence characteristics of conjugated organic molecules. I. Polyacenes, J. Mol. Struc.-Theochem, 2002, 585, 49-59.

[10] Narayan, M. R., Singh, J., Effect of exciton-spin-orbit-photon interaction in the performance of organic solar cells, Eur. Phys. J. B, 2013, 86, 47.

[11] Sheng, C. X., Singh, S., Gambetta, A., Drori, T., Tong, M., Tretiak, S., et al., Ultrafast intersystem-crossing in platinum containing pi-conjugated polymers with tunable spin-orbit coupling, Sci. Rep., 2013, 3, 2653.

[12] Schmidt, K., Brovelli, S., Coropceanu, V., Beljonne, D., Cornil, J., Bazzini, C., et al., Intersystem crossing processes in nonplanar aromatic heterocyclic molecules, J. Phys. Chem. A, 2007, 111, 10490-10499.

[13] Harmon, N. J., Flatte, M. E., Distinguishing Spin Relaxation Mechanisms in Organic Semiconductors, Phys. Rev. Lett., 2013, 110, 176602.

[14] Harmon, N. J., Flatte, M. E., Spin relaxation in materials lacking coherent charge transport, Phys. Rev. B, 2014, 90, 115203.

[15] Rybicki, J., Wohlgenannt, M., Spin-orbit coupling in singly charged pi-conjugated polymers, Phys. Rev. B, 2009, 79, 153202.

[16] Rybicki, J., Nguyen, T. D., Sheng, Y., Wohlgenannt, M., Spin-orbit coupling and spin relaxation rate in singly charged pi-conjugated polymer chains, Synth. Met., 2010, 160, 280-284.
[17] Khaetskii, A. V., Loss, D., Glazman, L., Electron spin decoherence in quantum dots due to interaction with nuclei, Phys. Rev. Lett., 2002, 88, 186802.
[18] Coish, W. A., Loss, D., Hyperfine interaction in a quantum dot: Non-Markovian electron spin dynamics, Phys. Rev. B, 2004, 70, 195340.
[19] Dyakonov, M. I., Spin Physics in Semiconductors, Springer Verlag, Berlin Heidelberg, 2008
[20] Steiner, U. E., Ulrich, T., Magnetic-field effects in chemical-kinetics and related phenomena, Chem. Rev., 1989, 89, 51-147.
[21] Frankevich, E., Balabanov, E., New effect of increasing photoconductivity of organic semiconductors in a weak magnetic field, JETP Lett.-USSR, 1965, 1, 169.
[22] Kalinowski, J., Cocchi, M., Virgili, D., Di Marco, P., Fattori, V., Magnetic field effects on emission and current in Alq(3)-based electroluminescent diodes, Chem. Phys. Lett., 2003, 380, 710-715.
[23] Francis, T. L., Mermer, O., Veeraraghavan, G., Wohlgenannt, M., Large magnetoresistance at room temperature in semiconducting polymer sandwich devices, New J. Phys., 2004, 6, 185.
[24] Mermer, O., Veeraraghavan, G., Francis, T. L., Sheng, Y., Nguyen, D. T., Wohlgenannt, M., et al., Large magnetoresistance in nonmagnetic pi-conjugated semiconductor thin film devices, Phys. Rev. B, 2005, 72, 205202.
[25] Koopmans, B., Wagemans, W., Bloom, F. L., Bobbert, P. A., Kemerink, M., Wohlgenannt, M., Spin in organics: a new route to spintronics, Philos. T. Roy. Soc. A, 2011, 369, 3602-3616.
[26] Wohlgenannt, M., Organic magnetoresistance and spin diffusion in organic semiconductor thin film devices. Phys. Status Solidi-R, 2012, 6, 229-242.
[27] Reichert, T., Saragi, T. P. I., Photoinduced magnetoresistance in organic field-effect transistors, Appl. Phys. Lett., 2011, 98, 063307.
[28] Nguyen, T. D., Hukic-Markosian, G., Wang, F., Wojcik, L., Li, X.-G., Ehrenfreund, E., et al., Isotope effect in spin response of pi-conjugated polymer films and devices, Nat. Mater., 2010, 9, 345-352.
[29] Nguyen, T. D., Basel, T. P., Pu, Y. J., Li, X. G., Ehrenfreund, E., Vardeny, Z. V., Isotope effect in the spin response of aluminum tris(8-hydroxyquinoline) based devices, Phys. Rev. B, 2012, 85, 245437.
[30] Malissa, H., Kavand, M., Waters, D. P., van Schooten, K. J., Burn, P. L., Vardeny, Z. V., et al., Room-temperature coupling between electrical current and nuclear spins in OLEDs, Science, 2014, 345, 1487-1490.
[31] Bobbert, P. A., Nguyen, T. D., van Oost, F. W. A., Koopmans, B., Wohlgenannt, M., Bipolaron mechanism for organic magnetoresistance, Phys. Rev. Lett., 2007, 99, 216801.
[32] Prigodin, V. N., Bergeson, J. D., Lincoln, D. M., Epstein, A. J., Anomalous room temperature magnetoresistance in organic semiconductors, Synth. Met., 2006, 156, 757-761.
[33] Desai, P., Shakya, P., Kreouzis, T., Gillin, W. P., Morley, N. A., Gibbs, M. R. J., Magnetoresistance and efficiency measurements of Alq(3)-based OLEDs, Phys. Rev. B, 2007, 75, 094423.
[34] Johnson, R. C., Merrifield, R. E., Avakian, P., Flippen, R. B., Effects of magnetic fields on mutual annihilation of triplet excitons in molecular crystals, Phys. Rev. Lett., 1967, 19, 285.
[35] Janssen, P., Cox, M., Wouters, S. H. W., Kemerink, M., Wienk, M. M., Koopmans, B., Tuning organic magnetoresistance in polymer-fullerene blends by controlling spin reaction pathways, Nat. Comm., 2013, 4, 2286.
[36] Gu, H., Kreouzis, T., Gillin, W. P., The transition from bipolaron to triplet-polaron magnetoresistance in a single layer organic semiconductor device, Org. Electron., 2014, 15, 1711-1716.
[37] Baker, W. J., Keevers, T. L., Lupton, J. M., McCamey, D. R., Boehme, C., Slow Hopping and Spin Dephasing of Coulombically Bound Polaron Pairs in an Organic Semiconductor at Room Temperature, Phys. Rev. Lett., 2012, 108, 267601.
[38] Maeda, K., Henbest, K. B., Cintolesi, F., Kuprov, I., Rodgers, C. T., Liddell, P. A., et al., Chemical compass model of avian magnetoreception, Nature, 2008, 453, 387-390.
[39] Engels, S., Schneider, N.-L., Lefeldt, N., Hein, C. M., Zapka, M., Michalik, A., et al., Anthropogenic electromagnetic noise disrupts magnetic compass orientation in a migratory bird, Nature, 2014, 509, 353-356.
[40] Tsymbal, E. Y., Mryasov, O. N., LeClair, P. R., Spin-dependent tunnelling in magnetic tunnel junctions, J. Phys.-Condens. Mat., 2003, 15, R109-R142.
[41] Chappert, C., Fert, A., Van Dau, F. N., The emergence of spin electronics in data storage, Nat. Mater., 2007, 6, 813-823.
[42] Awschalom, D. D., Flatte, M. E., Challenges for semiconductor spintronics, Nat. Phys. 2007, 3, 153-159.
[43] Fabian, J., Matos-Abiague, A., Ertler, C., Stano, P., Zutic, I., Semiconductor spintronics, Acta Phys. Slovaca, 2007, 57, 565-907.
[44] Dediu, V., Murgia, M., Matacotta, F. C., Taliani, C., Barbanera, S., Room temperature spin polarized injection in organic semiconductor, Solid State Commun., 2002, 122, 181-184.
[45] Xiong, Z. H., Wu, D., Vardeny, Z. V., Shi, J., Giant magnetoresistance in organic spin-valves, Nature, 2004, 427, 821-824.
[46] Dediu, V. A., Hueso, L. E., Bergenti, I., Taliani, C., Spin routes in organic semiconductors, Nat. Mater. 2009, 8, 707-716.
[47] Naber, W. J. M., Faez, S., van der Wiel, W. G., Organic spintronics, J. Phys. D-Appl. Phys., 2007, 40, R205-R228.
[48] Ouyang, M., Awschalom, D. D., Coherent spin transfer between molecularly bridged quantum dots, Science, 2003, 301, 1074-1078.
[49] Petta, J. R., Slater, S. K., Ralph, D. C., Spin-dependent transport in molecular tunnel junctions, Phys. Rev. Lett. 2004, 93, 136601.
[50] Wang, W., Richter, C. A., Spin-polarized inelastic electron tunneling spectroscopy of a molecular magnetic tunnel junction, Appl. Phys. Lett., 2006, 89, 153105.
[51] Galbiati, M., Barraud, C., Tatay, S., Bouzehouane, K., Deranlot, C., Jacquet, E., et al., Unveiling Self-Assembled Monolayers' Potential for Molecular Spintronics: Spin Transport at High Voltage, Adv. Mater., 2012, 24, 6429-6432.
[52] Santos, T. S., Lee, J. S., Migdal, P., Lekshmi, I. C., Satpati, B., Moodera, J. S., Room-temperature tunnel magnetoresistance and spin-polarized tunneling through an organic semiconductor barrier, Phys. Rev. Lett., 2007, 98, 016601.
[53] Schoonus, J. J. H. M., Lumens, P. G. E., Wagemans, W., Kohlhepp, J. T., Bobbert, P. A., Swagten, H. J. M., et al., Magnetoresistance in Hybrid Organic Spin Valves at the Onset of Multiple-Step Tunneling, Phys. Rev. Lett. 2009, 103, 146601.
[54] Tran, T. L. A., Le, T. Q., Sanderink, J. G. M., van der Wiel, W. G., de Jong, M. P., The Multistep Tunneling Analogue of Conductiv-

ity Mismatch in Organic Spin Valves, Adv. Funct. Mater., 2012, 22, 1180-1189.

[55] Roundy, R. C., Raikh, M. E., Tunnel magnetoresistance in organic spin valves in the regime of multistep tunneling, Phys. Rev. B, 2013, 88, 205206.

[56] Roundy, R. C., Nemirovsky, D., Kagalovsky, V., Raikh, M. E., Giant Fluctuations of Local Magnetoresistance of Organic Spin Valves and the Non-Hermitian 1D Anderson Model, Phys. Rev. Lett., 2014, 112, 226601.

[57] Barraud, C., Seneor, P., Mattana, R., Fusil, S., Bouzehouane, K., Deranlot, C., et al., Unravelling the role of the interface for spin injection into organic semiconductors, Nat. Phys. 2010, 6, 615-620.

[58] Lin, R., Wang, F., Rybicki, J., Wohlgenannt, M., Hutchinson, K. A., Distinguishing between tunneling and injection regimes of ferromagnet/organic semiconductor/ferromagnet junctions, Phys. Rev. B, 2010, 81, 195214.

[59] Sun, X., Gobbi, M., Bedoya-Pinto, A., Txoperena, O., Golmar, F., Llopis, R., et al., Room-temperature air-stable spin transport in bathocuproine-based spin valves, Nat. Commun., 2013, 4, 2794.

[60] Li, F., Li, T., Chen, F., Zhang, F., Spin injection and transport in organic spin-valves based on fullerene C-60, Org. Electron., 2014, 15, 1657-1663.

[61] Zhan, Y. Q., de Jong, M. P., Li, F. H., Dediu, V., Fahlman, M., Salaneck, W. R., Energy level alignment and chemical interaction at Alq(3)/Co interfaces for organic spintronic devices, Phys. Rev. B, 2008, 78, 045208.

[62] Borgatti, F., Bergenti, I., Bona, F., Dediu, V., Fondacaro, A., Huotari, S., et al., Understanding the role of tunneling barriers in organic spin valves by hard x-ray photoelectron spectroscopy, Appl. Phys. Lett., 2010, 96, 043306.

[63] Wei, D. H., Wang, C.-H., Chang, H.-C., Chan, Y.-L., Lee, C.-H., Hsu, Y.-J., Direct imaging and spectral identification of the interfaces in organic semiconductor-ferromagnet heterojunction, Appl. Phys. Lett., 2012, 101, 141605.

[64] Cheng, P. Y., Chiang, M. R., Chan, Y. L., Hsu, Y. J., Wang, P. C., Wei, D. H., Deep Co penetration and spin-polarization of C-60 molecules at hybridized Co-C-60 interfaces, Appl. Phys. Lett., 2014, 104, 043303.

[65] Dediu, V., Hueso, L. E., Bergenti, I., Riminucci, A., Borgatti, F., Graziosi, P., et al., Room-temperature spintronic effects in Alq3-based hybrid devices, Phys. Rev. B, 2008, 78, 115203.

[66] Sun, D., Yin, L., Sun, C., Guo, H., Gai, Z., Zhang, X. G., et al., Giant Magnetoresistance in Organic Spin Valves, Phys. Rev. Lett., 2010, 104, 236602.

[67] Prezioso, M., Riminucci, A., Graziosi, P., Bergenti, I., Rakshit, R., Cecchini, R., et al., A Single-Device Universal Logic Gate Based on a Magnetically Enhanced Memristor, Adv. Mater., 2013, 25, 534-538.

[68] Daalderop, G. H. O., Kelly, P. J., Schuurmans, M. F. H., 1st-principles calculation of the magnetocrystalline anisotropy energy of iron, cobalt, and nickel, Phys. Rev. B, 1990, 41, 11919-11937.

[69] Gould, C., Ruster, C., Jungwirth, T., Girgis, E., Schott, G. M., Giraud, R., et al., Tunneling anisotropic magnetoresistance: A spin-valve-like tunnel magnetoresistance using a single magnetic layer, Phys. Rev. Lett., 2004, 93, 117203.

[70] Gruenewald, M., Wahler, M., Schumann, F., Michelfeit, M., Gould, C., Schmidt, R., et al., Tunneling anisotropic magnetoresistance in organic spin valves, Phys. Rev. B, 2011, 84, 125208.

[71] Wang, K., Sanderink, J. G. M., Bolhuis, T., van der Wiel, W. G., de Jong, M. P., Tunneling anisotropic magnetoresistance in C-60-based organic spintronic systems, Phys. Rev. B, 2014, 89, 174419.

[72] Wang, K., Tran, T. L. A., Brinks, P., Sanderink, J. G. M., Bolhuis, T., van der Wiel, W. G., et al., Tunneling anisotropic magnetoresistance in Co/AlOx/Al tunnel junctions with fcc Co (111) electrodes, Phys. Rev. B, 2013, 88, 054407.

[73] Ruden, P. P., Smith, D. L., Theory of spin injection into conjugated organic semiconductors, J. Appl. Phys., 2004, 95, 4898-4904.

[74] Goswami, A., Yunus, M., Ruden, P. P., Smith, D. L., Magnetoresistance of organic spin valves due to spin-polarized tunnel injection and extraction of charge carriers, J. Appl. Phys., 2012, 111, 034505.

[75] Shumilin, A. V., Kabanov, V. V., Dediu, V. A., Magnetoresistance in organic spintronic devices: the role of nonlinear effects, New J. Phys., 2015, 17, 023019.

[76] Drew, A. J., Hoppler, J., Schulz, L., Pratt, F. L., Desai, P., Shakya, P., et al., Direct measurement of the electronic spin diffusion length in a fully functional organic spin valve by low-energy muon spin rotation, Nat. Mater., 2009, 8, 109-114.

[77] Cinchetti, M., Heimer, K., Wuestenberg, J.-P., Andreyev, O., Bauer, M., Lach, S., et al., Determination of spin injection and transport in a ferromagnet/organic semiconductor heterojunction by two-photon photoemission, Nat. Mater., 2009, 8, 115-119.

[78] Lou, X., Adelmann, C., Crooker, S. A., Garlid, E. S., Zhang, J., Reddy, K. S. M., et al., Electrical detection of spin transport in lateral ferromagnet-semiconductor devices, Nat. Phys., 2007, 3, 197-202.

[79] Huang, B., Monsma, D. J., Appelbaum, I., Coherent spin transport through a 350 micron thick silicon wafer, Phys. Rev. Lett., 2007, 99, 177209.

[80] Johnson, M., Silsbee, R. H., Interfacial charge-spin coupling - Injection and detection of spin magnetization in metals, Phys. Rev. Lett., 1985, 55, 1790-1793.

[81] Johnson, M., Silsbee, R. H., Spin-injection experiment, Phys. Rev. B ,1988, 37, 5326-5335.

[82] Yang, H., Yang, S. H., Takahashi, S., Maekawa, S., Parkin, S. S. P., Extremely long quasiparticle spin lifetimes in superconducting aluminium using MgO tunnel spin injectors, Nat. Mater., 2010, 9, 586-593.

[83] Riminucci, A., Prezioso, M., Pernechele, C., Graziosi, P., Bergenti, I., Cecchini, R., et al., Hanle effect missing in a prototypical organic spintronic device, Appl. Phys. Lett., 2013, 102, 092407.

[84] Gruenewald, M., Goeckeritz, R., Homonnay, N., Wuerthner, F., Molenkamp, L. W., Schmidt, G., Vertical organic spin valves in perpendicular magnetic fields, Phys. Rev. B, 2013, 88, 085319.

[85] Yu, Z. G., Suppression of the Hanle Effect in Organic Spintronic Devices, Phys. Rev. Lett. 2013, 111, 016601.

[86] Tserkovnyak, Y., Brataas, A., Bauer, G. E. W., Enhanced Gilber damping in thin ferromagnetic films, Phys. Rev. Lett., 2002, 88, 117601.

[87] Watanabe, S., Ando, K., Kang, K., Mooser, S., Vaynzof, Y., Kurebayashi, H., et al., Polaron spin current transport in organic semiconductors, Nat. Phys., 2014, 10, 308-313.

[88] Sanvito, S., Molecular Spintronics: The rise of spinterface science, Nat. Phys., 2010, 6, 562-564.
[89] Atodiresei, N., Brede, J., Lazic, P., Caciuc, V., Hoffmann, G., Wiesendanger, R., et al., Design of the Local Spin Polarization at the Organic-Ferromagnetic Interface, Phys. Rev. Lett., 2010, 105, 066601.
[90] Kawahara, S. L., Lagoute, J., Repain, V., Chacon, C., Girard, Y., Rousset, S., et al., Large Magnetoresistance through a Single Molecule due to a Spin-Split Hybridized Orbital, Nano Lett., 2012, 12, 4558-4563.
[91] Al Ma'Mari, F., Moorsom, T., Teobaldi, G., Deacon, W., Prokscha, T., Luetkens, H., et al., Beating the Stoner criterion using molecular interfaces, Nature, 2015, 524, 69-73.
[92] Raman, K. V., Kamerbeek, A. M., Mukherjee, A., Atodiresei, N., Sen, T. K., Lazic, P., et al., Interface-engineered templates for molecular spin memory devices, Nature, 2013, 493, 509-513.
[93] Rizzini, A. L., Krull, C., Mugarza, A., Balashov, T., Nistor, C., Piquerel, R., et al., Coupling of single, double, and triple-decker metal-phthalocyanine complexes to ferromagnetic and antiferromagnetic substrates, Surf. Sci., 2014, 630, 361-374.
[94] Tran, T. L. A., Wong, P. K. J., de Jong, M. P., van der Wiel, W. G., Zhan, Y. Q., Fahlman, M., Hybridization-induced oscillatory magnetic polarization of C-60 orbitals at the C-60/Fe(001) interface, Appl. Phys. Lett., 2011, 98, 222505.
[95] Tran, T. L. A., Cakir, D., Wong, P. K. J., Preobrajenski, A. B., Brocks, G., van der Wiel, W. G., et al., Magnetic Properties of bcc-Fe(001)/C-60 Interfaces for Organic Spintronics, ACS Appl. Mater. Inter., 2013, 5, 837-841.
[96] Schmaus, S., Bagrets, A., Nahas, Y., Yamada, T. K., Bork, A., Bowen, M., et al., Giant magnetoresistance through a single molecule, Nat. Nanotech., 2011, 6, 185-189.
[97] Brede, J., Atodiresei, N., Kuck, S., Lazic, P., Caciuc, V., Morikawa, Y., et al., Spin- and Energy-Dependent Tunneling through a Single Molecule with Intramolecular Spatial Resolution, Phys. Rev. Lett., 2010, 105, 047204.
[98] Chu, Y.-H., Hsu, C.-H., Lu, C.-I., Yang, H.-H., Yang, T.-H., Luo, C.-H., et al., Spin-Dependent Molecule Symmetry at a Pentacene-Co Spinterface, ACS Nano, 2015, 9, 7027-7032.
[99] Suzuki, T., Kurahashi, M., Ju, X., Yamauchi, Y., Spin polarization of metal (Mn, Fe, Cu, and Mg) and metal-free phthalocyanines on an Fe(100) substrate, J. Phys. Chem. B, 2002, 106, 11553-11556.
[100] Suzuki, T., Kurahashi, M., Yamauchi, Y., Spin polarization in molecular orbitals of copper-phthalocyanine deposited on a magnetized Fe(100) substrate, J. Phys. Chem. B, 2002, 106, 7643-7646.
[101] Suzuki, T., Kurahashi, M., Ju, X., Yamauchi, Y., Adsorption structure and spin polarization of pentacene on a magnetized Fe(100) substrate: SPMDS and ERDA study, Surf. Sci., 2004, 549, 97-102.
[102] Wisbey, D., Wu, N., Feng, D., Caruso, A. N., Belot, J., Losovyj, Y., et al., Interface-induced spin and dipole ordering of the copper spin 1/2 molecule: Bis(4-cyano-2,2,6,6-tetramethyl-3,5-heptanedionato)copper(II), J. Phys. Chem. C, 2008, 112, 13656-13662.
[103] Lach, S., Altenhof, A., Tarafder, K., Schmitt, F., Ali, M. E., Vogel, M., et al., Metal-Organic Hybrid Interface States of A Ferromagnet/Organic Semiconductor Hybrid Junction as Basis For Engineering Spin Injection in Organic Spintronics, Adv. Funct. Mater., 2012, 22, 989-997.
[104] Djeghloul, F., Ibrahim, F., Cantoni, M., Bowen, M., Joly, L., Boukari, S., et al., Direct observation of a highly spin-polarized organic spinterface at room temperature, Sci. Rep., 2013, 3, 1272.
[105] Oppeneer, P. M., Panchmatia, P. M., Sanyal, B., Eriksson, O., Ali, M. E., Nature of the magnetic interaction between Fe-porphyrin molecules and ferromagnetic surfaces, Prog. Surf. Sci., 2009, 84, 18-29.
[106] Atodiresei, N., Caciuc, V., Lazic, P., Bluegel, S., Engineering the magnetic properties of hybrid organic-ferromagnetic interfaces by molecular chemical functionalization, Phys. Rev. B, 2011, 84, 172402.
[107] Ali, M. E., Sanyal, B., Oppeneer, P. M., Tuning the Magnetic Interaction between Manganese Porphyrins and Ferromagnetic Co Substrate through Dedicated Control of the Adsorption, J. Phys. Chem. C, 2009, 113, 14381-14383.
[108] Friedrich, R., Caciuc, V., Kiselev, N. S., Atodiresei, N., Bluegel, S., Chemically functionalized magnetic exchange interactions of hybrid organic-ferromagnetic metal interfaces, Phys. Rev. B, 2015, 91, 115432.
[109] Lazic, P., Caciuc, V., Atodiresei, N., Callsen, M., Bluegel, S., First-principles insights into the electronic and magnetic structure of hybrid organic-metal interfaces, J. Phys.-Condens. Mat., 2014, 26, 263001.
[110] Przybylski, M., Gradmann, U., Ferromagnetic order in a Fe(110) monolayer on W(110) by Mossbauer-spectroscopy, Phys. Rev. Lett., 1987, 59, 1152-1155.
[111] Barraud, C., Bouzehouane, K., Deranlot, C., Fusil, S., Jabbar, H., Arabski, J., et al., Unidirectional Spin-Dependent Molecule-Ferromagnet Hybridized States Anisotropy in Cobalt Phthalocyanine Based Magnetic Tunnel Junctions, Phys. Rev. Lett., 2015, 114, 206603.
[112] Spisak, D., Hafner, J., Diffusion of Fe atoms on W surfaces and Fe/W films and along surface steps, Phys. Rev. B, 2004, 70, 195426.
[113] Moorsom, T., Wheeler, M., Khan, T. M., Al Ma'Mari, F., Kinane, C., Langridge, S., et al., Spin-polarized electron transfer in ferromagnet/C-60 interfaces, Phys. Rev. B, 2014, 90, 125311.
[114] Bairagi, K., Bellec, A., Repain, V., Chacon, C., Girard, Y., Garreau, Y., et al., Tuning the Magnetic Anisotropy at a Molecule-Metal Interface, Phys. Rev. Lett., 2015, 114, 247203.